

Cartesian Impedance Control Techniques for Torque Controlled Light-Weight Robots

Alin Albu-Schäffer

Gerd Hirzinger

DLR Oberpfaffenhofen
German Aerospace Research Center
Institute of Robotics and Mechatronics
Alin.Albu-Schaeffer@dlr.de, Gerd.Hirzinger@dlr.de

Abstract

The paper compares various approaches to implementing a compliant Cartesian behavior for robotic manipulators: impedance, admittance and stiffness control. A new controller structure is proposed, which consists of an impedance controller enhanced by local stiffness control. This structure consistently takes into account the two time scale property of the joint and Cartesian control loops. The DLR light-weight robot, with its position, torque and impedance interfaces on joint level, is an adequate platform for the implementation of the presented methods. The experimental results are discussed and a critical comparison of the performance with different controllers is made. As an application for the new control structure, the fast and intuitive teaching of an insertion task (piston into a motor block) is described.

1 Introduction

Applications in which a robot's end-effector interacts with the environment require a suitable compliant behavior to be implemented in Cartesian space. A well established framework to manage this task is given by impedance control [8]. The aim of an impedance controller is to establish a mass-damper-spring relationship between the Cartesian position Δx and the Cartesian force f :

$$f = M\Delta\ddot{x} + D_k\Delta\dot{x} + K_k\Delta x, \quad (1)$$

where M , D_k and K_k are positive definite matrices representing the virtual inertia, damping and stiffness of the system. If the focus is on the stiffness and damping properties, there exist various control strategies to implement this behavior on a real robot system. In this paper we will focus on admittance control, impedance control and stiffness control. The first method is widely used, since a position control interface is available on every robotic system. In contrast, the last two methods require a joint torque or

joint impedance interface. The usefulness of direct current command as a torque interface is limited for most robots by the disturbing influence of the friction. The joints of the DLR light-weight robots are equipped with torque sensors, enabling joint position, torque and stiffness control. Thus, they are an adequate platform for the implementation and comparison of the aforementioned Cartesian control methods [7]. An overview of the controller architecture of the DLR robots is given in section 2.

The paper first considers the classical structures of admittance, impedance and stiffness control, with a special focus on the last method, which is quite common for robotic hands but rarely used for arms. It turns out that stiffness control leads to substantial geometrical errors for high displacements. The use of a conservative congruence transformation does not improve the results considerably. In this paper we propose a new control strategy, which consists in impedance control augmented by local stiffness control. This approach combines the benefits of both control methods in terms of geometric accuracy and attainable stiffness range.

2 Overview of the LWR controller architecture

Fig. 1 gives an overview of the controller structure implemented on DLR's light-weight robots. The joint control is computed in a decentralized manner, on a signal processor in each joint, with a sampling rate of 3kHz. A flexible joint model is assumed for the robots [3]. The motor position q_1 and joint torque τ are available from measurements. Their derivatives are computed numerically. With these four signals it is possible to implement joint controllers with full state feedback.

Conditions for the passivity of the controllers were derived in [2]. The joint controller is actually an impedance controller, which, depending on the commanded joint stiffness, can be parameterized as a po-

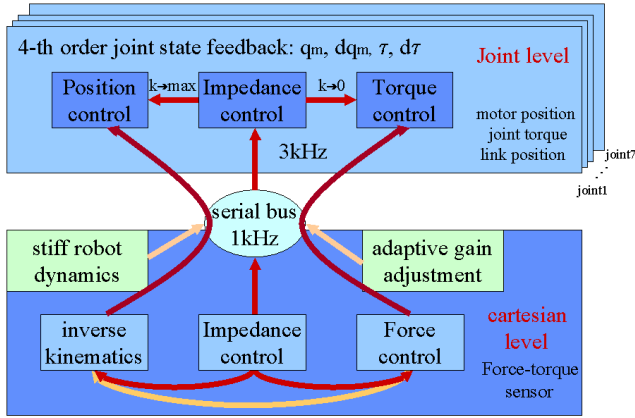


Figure 1: Controller architecture for DLR’s light-weight robots

sition controller ($k_{des} = k_{max}$) or a torque controller ($k_{des} \rightarrow 0$). Every 1ms the joints receive the desired values $\{\dot{q}_{1d}, q_{1d}, \dot{\tau}_d, \tau_d\}$, the variable parameters for the joint controllers as well as a feed-forward motor torque command term from the central robot controller. The measured values are transmitted with the same sampling rate from the joints to the Cartesian level.

The robot dynamics, the kinematics and the inverse kinematics are computed in the central robot controller. In every Cartesian cycle the gains for the joint controllers are also computed as a function of the desired stiffness and the current value of the inertia matrix.

This structure is well suited for the implementation and testing of various Cartesian control strategies. For example, the Cartesian force controller can be implemented either by using the transposed Jacobian and accessing the joint torque interface, or by using the inverse kinematics and accessing the joint position interface. In a similar way, the structure can be used to implement admittance, impedance and stiffness control.

3 Impedance control methods

In this section we summarize the three aforementioned control methods, which can be used to obtain the desired compliant robot behavior in Cartesian space. Therefore it is useful to keep in mind that regardless of the control method, the motor torque is eventually the value commanded to the robot.

3.1 Admittance Control

The Cartesian force at the end-effector is measured in the case of admittance control by a 6DOF force-torque sensor. The force vector is used to generate a desired Cartesian position x_d . Using the inverse kinematics \mathcal{K}^{-1} , this displacement is converted to desired

joint positions. The joint position controller $\mathcal{P}_{\mathcal{R}}$ then generates the motor torques:

$$x_d(s) = x_0(s) - \frac{\Delta f(s)}{K_k + D_k s} \rightarrow q_{2d} = \mathcal{K}^{-1}\{x_d\} \rightarrow \tau_m = \mathcal{P}_{\mathcal{R}}\{q_{2d}\} \quad (2)$$

where q_2 is the link side position of the joints. This method is the most commonly used one, since most robots have only a position interface. The advantages are that the high gain position controllers can compensate for the friction in the joints and that, for the implementation of high stiffness, low gains are needed in the Cartesian control loop. Hence it is clear that stability problems will appear for low desired stiffness and damping, for which the bandwidth of the Cartesian control loop approaches the joint bandwidth. This problem is even more noticeable for flexible joint robots, since in that case the bandwidth of joint control is more critical. Further problems arise in the vicinity of singularities, where Cartesian position control can typically lead to fast, destabilizing movements.

3.2 Impedance Control

The impedance control uses directly the equation (1), in which the actual Cartesian position $x = \mathcal{K}(q_2)$ is computed from the position q_2 using direct kinematics. Using the transposed Jacobian $J^T(q_2)$, the Cartesian force is transformed into desired joint torques. The joint torque controller $\mathcal{T}_{\mathcal{R}}$ then generates the motor torque command:

$$f = K_k \Delta x + D_k \Delta \dot{x} \rightarrow \tau_d = J^T(q_2) f \rightarrow \tau_m = \mathcal{T}_{\mathcal{R}}\{\tau_d\} \quad (3)$$

To obtain good results with this method, a joint torque controller which can overcome the joint friction disturbance is very useful. The impedance controller is, in principle, complementary to the admittance controller. It is well suited for low stiffness and damping, which now require low gains in the Cartesian loop, while the bandwidth of the torque controller is optimally exploited. The stability problems will appear correspondingly for high Cartesian stiffness.

The behavior at singularities is also different from that of the admittance controller. Components of f , which act in singular directions, are not mapped to the joint space. The movement in the vicinity of singularities will be stable and smooth, but the stiffness matrix will be distorted.

3.3 Stiffness control

From the previous two methods one can see that appropriate performance can be achieved if the gains

in the Cartesian control loop are substantially lower than those in the joint controllers. This leads to the idea of converting the desired Cartesian stiffness and damping to corresponding matrices for the joint stiffness K_j and damping D_j . Assuming that the desired Cartesian matrices are changing rather slowly, there is no need for very high Cartesian sampling rates. The joint impedance controller $\mathcal{S}_{\mathcal{R}}$ can then be used to generate the desired motor torque.

$$\begin{aligned} \{K_j, D_j\} &= \mathcal{T}\{K_k, D_k\} \rightarrow \\ \rightarrow \tau_m &= \mathcal{S}_{\mathcal{R}}\{\mathcal{K}^{-1}(x_d), K_j, D_j\} \end{aligned} \quad (4)$$

3.4 Limitations of the stiffness controller

The mapping \mathcal{T} as well as the matrices $\{K_j, D_j\}$ have only a local meaning. K_j and D_j give a local relationship between the joint torque and the joint position or the joint velocities, respectively.

$$\begin{aligned} D_j &= \frac{\partial \tau}{\partial \dot{q}_2^T} = \frac{\partial (J(q_2)^T D_k \Delta \dot{x})}{\partial \dot{q}_2^T} = J(q_2)^T D_k J(q_2) \\ K_j &= \frac{\partial \tau}{\partial q_2^T} = \frac{\partial (J(q_2)^T K_k \Delta x)}{\partial q_2^T} \\ &= J(q_2)^T K_k J(q_2) + \frac{\partial J(q_2)^T}{\partial q_2^T} K_k \Delta x \end{aligned} \quad (5)$$

¹ In the early work of [14], only the first term of (5) is mentioned. The importance of the second term, which reflects the position dependent change of the Jacobian is pointed out in [9, 5, 6, 1]. The idea of mapping the Cartesian stiffness to the joint stiffness is biologically motivated. The human arm is able to change its stiffness by contracting antagonistic muscle pairs [9, 12]. In case of robotic manipulators, this can be accomplished only by means of control, the input for the robot is always the motor torque.

The direct implementation of a Cartesian stiffness with the control law:

$$\tau_d = K_j(\mathcal{K}^{-1}\{x_0\} - q_2) - D_j \dot{q}_2 \quad (6)$$

leads, at least for higher displacements Δx from the desired position, to substantial errors in the stiffness matrix. The reason for these errors is the local character of (5). The last term in (5) does not completely eliminate this error, because $\frac{\partial (K_k \Delta x)}{\partial q} = K_k J(q_2)$ is also valid only locally. Here, the Jacobian is implicitly

¹For sake of simplicity, we used here the somewhat sloppy expression from [9] of the derivative of a matrix by a vector $\frac{\partial (J(q_2))}{\partial q^T}$. Writing the expression for every row of K_{j_i} with $i = 1, \dots, N$ eliminates the ambiguity. The resulting matrix is of course equivalent also to the formulation of the conservative congruence transformation in [5, 6].

assumed to be constant, despite of being multiplied by a big displacement Δq_2 .

4 Impedance controller enhanced by local stiffness control

In this section, a new controller structure for the implementation of Cartesian stiffness is presented. Based on the remarks in the previous section, the new controller structure is designed with the following considerations in mind:

- (A1) $J(q_2)$ and $x = \mathcal{K}(q_2)$ may be computed in a slower Cartesian control loop.
- (A2) The robot has a fast joint control loop, for which the time delay is negligible, so that $q_2 \approx q_{2j}$.
- (A3) (6) is valid only locally.

Notations: The signals, which are measured or computed in the Cartesian loop are denoted by the index $[\]_k$. The index $[\]_j$ refers to signals determined in the joint control loop, while the real (instantaneous) values have no index. Furthermore, for the difference signals, the notations $\Delta q_k = q_0 - q_k$ and $\Delta q_j = q_k - q_j$ are used. Considering (A1), it follows that :

$$\begin{aligned} \Delta x &= x_0 - x \approx x_0 - x_k - \left. \frac{\partial x}{\partial q_2^T} \right|_{q_2=q_{2k}} (q_{2j} - q_{2k}) = \\ &= \Delta x_k + J(q_{2k}) \Delta q_{2j} \end{aligned} \quad (7)$$

$$J^T(q_2) \approx J^T(q_{2j}) \approx J^T(q_{2k}) + \Delta q_{2j}^T \left. \frac{\partial J^T(q_2)}{\partial q_2} \right|_{q_2=q_{2k}} \quad (8)$$

This leads to the following expression for the stiffness induced component of the desired joint torque:

$$\begin{aligned} \tau_{dK} &= J^T(q_2) K_k \Delta x = J^T(q_{2k}) K_k \Delta x_k + \\ &+ J^T(q_{2k}) K_k J(q_{2k}) \Delta q_{2j} + \\ &+ \Delta q_{2j}^T \left. \frac{\partial J^T(q_2)}{\partial q_2} \right|_{q_2=q_{2k}} K_k \Delta x_k + \\ &+ \Delta q_{2j}^T \left. \frac{\partial J^T(q_2)}{\partial q_2} \right|_{q_2=q_{2k}} K_k J(q_{2k}) \Delta q_{2j} \end{aligned} \quad (9)$$

The first term corresponds to the impedance controller on Cartesian level. The second term corresponds to the stiffness controller, as described in [14]. Here, in contrast to (6), the stiffness controller acts only locally, in the vicinity of the last Cartesian position. This helps overcoming the slower Cartesian sampling rate by the faster joint controller.

The third term corresponds to the correction term in (5), which ensures the conservativeness of the mapping. Since the term contains the Cartesian elastic force for the complete displacement $K_k \Delta x_k$, it can not always be ignored, although the variation of the

Jacobian within a Cartesian cycle is small. Finally, the fourth term depends on the square of the small displacement Δq_{2j} and consequently has no practical significance.

In a similar way one obtains for the damping term:

$$\begin{aligned} \tau_{dD} = & J^T(q_{2k})D_kJ(q_{2k})\Delta\dot{q}_{2j} + \\ & + \Delta q_{2j}^T \frac{\partial J(q_2)^T}{\partial q_2} \Big|_{q_2=q_{2k}} D_kJ(q_{2k})\Delta\dot{q}_{2j} \quad (10) \end{aligned}$$

The second term in this expression may again be ignored.

The desired torque $\tau_d = \tau_{dK} + \tau_{dD}$ can be commanded to the torque controller. To exploit the performance of the joint controller optimally, it is more advantageous to use the joint stiffness controller instead. The term $J^T(q_{2k})K_k\Delta x_k$ is computed in the Cartesian loop and is sent as a commanded torque value to the stiffness controller. The terms $J^T(q_{2k})K_kJ(q_{2k})$ and $\frac{\partial J(q_2)^T}{\partial q_2} \Big|_{q_2=q_{2k}} K_k\Delta x$ are also computed in every Cartesian cycle and represent a constant desired stiffness, which is commanded to the joint controllers for the duration of this step.

Remark: In the current, decentralized joint controller structure, only the diagonal terms of the stiffness and damping matrices can be implemented using the joint impedance controller. The torques produced by the off-diagonal elements are computed on the central computer in a joint level task (at the bus sampling rate of 1ms) and are added to the desired torques.

5 Experimental results

The controller structures, which were described in sec. 3 and sec. 4, have been implemented on the DLR light-weight robots. In this section an experiment is described, which compares the performance of the various controllers. During the experiment, the desired position is kept constant. A very low stiffness is commanded in one translational direction (y), while the desired stiffness in the other Cartesian directions is high. Regardless of the forces applied by the user hand at the end-effector, the robot should consequently be able to move only in the y-direction. The controllers are compared in terms of the minimal and maximal stiffness that can be achieved, as well as in terms of the geometric accuracy for high displacements. The commanded values for the stiffness are summarized in table 1.

Table 1: Commanded values for the diagonal Cartesian stiffness matrix

x	y	z	roll ²	pitch	yaw
3000	100	3000	200	200	200
N/m	N/m	N/m	Nm/rad	Nm/rad	Nm/rad

The pure impedance controller showed up the poorest performance in terms of achievable stiffness range. As expected, it was not possible to implement high stiffness with this controller. The stiffness for which stability was preserved, was by a factor of 10 lower than for the other controllers. Reasons for this are the high gains needed in the Cartesian control loop and the limited bandwidth of the joint torque controller. Closing the impedance control loop on Cartesian level leads to a cascaded structure. For high stiffness, the separation principle for the time constants of the two stages of the cascade is violated. A comparison between the impedance controller and other structures from the point of view of geometric accuracy was therefore not possible.

The stiffness controller implemented with (6),(5) shows up very good stiffness and damping range performances. Since the stiffness and the damping are implemented inside the fast joint controllers, it was possible to vary the stiffness from zero (torque control) to high values in the range of the position controller. Moreover, typical stability problems encountered by force controlled robots at contacts with hard surfaces were absent here, even for high velocity impacts. An important drawback of the method is, however, the poor performance in terms of geometric accuracy for high displacements. As it can be seen in fig. 2 and fig. 3, the trajectory described by the robot corresponds to the desired straight line only in a vicinity of the desired position, but becomes curved for higher displacements. In these positions, the Cartesian stiffness matrix is very distorted, for reasons presented in section 3.4. This effect was not substantially influenced by the use of a conservative or nonconservative congruence transformation. This fact severely limits the practical applicability of the method.

The other two curves in fig. 2 and fig. 3 present the results for the impedance controller enhanced by local stiffness control (section 4), with conservative and nonconservative congruence transformation. Due to the use of the impedance controller, the geometric accuracy is considerably improved, while the stability problems with the impedance controller are eliminated by the fast joint stiffness control. The advantages of a high stiffness range and a high bandwidth are preserved. Fig. 4 and fig. 5 show the measurements for the same controller together with the field of forces applied by the user and measured by a 6DOF force-

²Since the focus of this work is on the structures of the impedance controller, the values for the rotational stiffness were deliberately chosen high, so that the particular representation of orientations has no significant effects on the results, as pointed out in [4, 16].

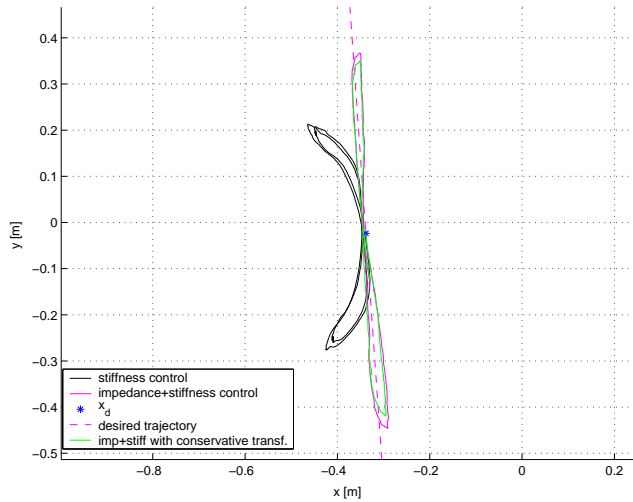


Figure 2: Measurements for stiffness control and impedance control enhanced by local stiffness control: x-y plot.

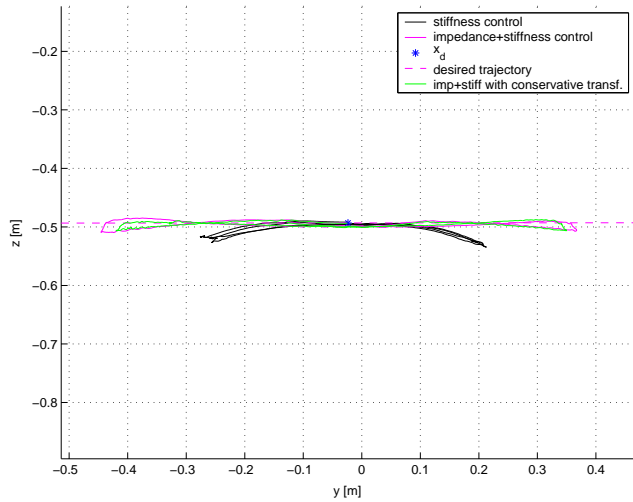


Figure 3: Measurements for stiffness control and impedance control enhanced by local stiffness control: y-z plot.

torque sensor. (Notice that in this case, the force sensor is used only for displaying the forces, the controller itself needs only joint position and joint torque measurements.) Fig. 4 also shows the robot in the initial configuration (x_0).

Finally, fig. 6 and fig. 7 compare the performance of the admittance controller with that of the controller from section 4. It can be seen that from respect to geometric accuracy, the admittance controller still has the best performance. This can be explained by the fact that the method explicitly uses inverse kinematics and that the high gains of the position controller compensate for the effects of friction.

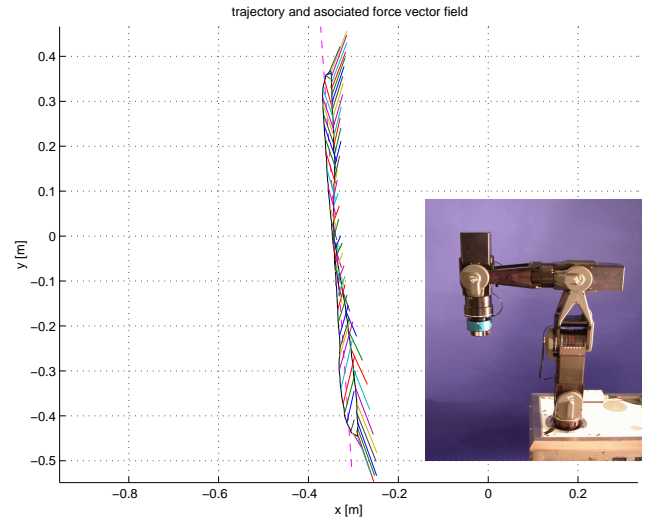


Figure 4: Measurements for impedance control enhanced by local stiffness control (x-y plot), together with the field of forces applied by the user

Nevertheless, the admittance controller also has some drawbacks compared to the controller from section 4. An important one is related to the behavior in the vicinity of singularities. Since in this situation inverse kinematics may lead to high joint velocity, the admittance controller tends to become unstable. In contrast, the other controller decreases its sensitivity, since forces at the end-effector can not be measured by the joint torque sensors. The controller remains stable, only the Cartesian stiffness matrix is distorted. Another drawback is related to the bandwidth of the admittance controller. Low stiffness can be achieved only if damping is considerably increased, still leading to a low bandwidth of the force controller implemented on the Cartesian level. This leads to stability problems at contact or impact with hard surfaces, unless the velocity of the robot is considerably reduced.

As a conclusion it can be stated that admittance control is a good choice for applications where geometric accuracy is relevant and the contacted environment does not have a very high stiffness. This is, for example, the case for force-feedback applications [13]. In applications where a high bandwidth is more important, while geometric accuracy is required only in a fairly large vicinity of the desired position, the impedance controller enhanced by local stiffness control is a better choice.

5.1 The behavior in the null-space

The DLR light-weight robots are 7DOF redundant manipulators [7]. The control methods presented above are influencing only the TCP behavior of the robot [11]. The explicit control of the robot motion in

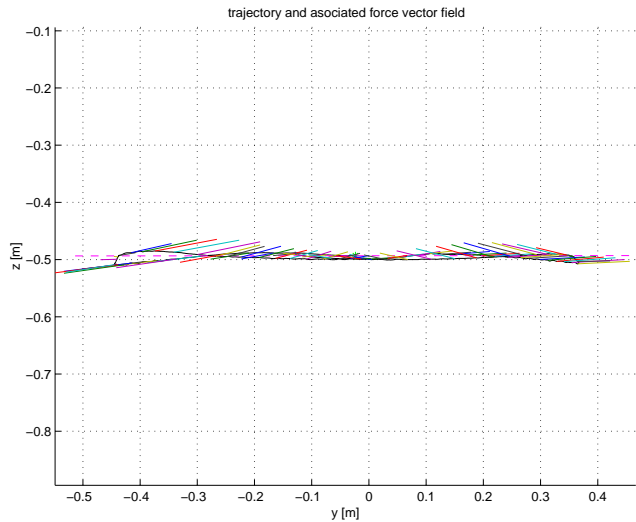


Figure 5: Measurements for impedance control enhanced by local stiffness control (y-z plot), together with the field of forces applied by the user

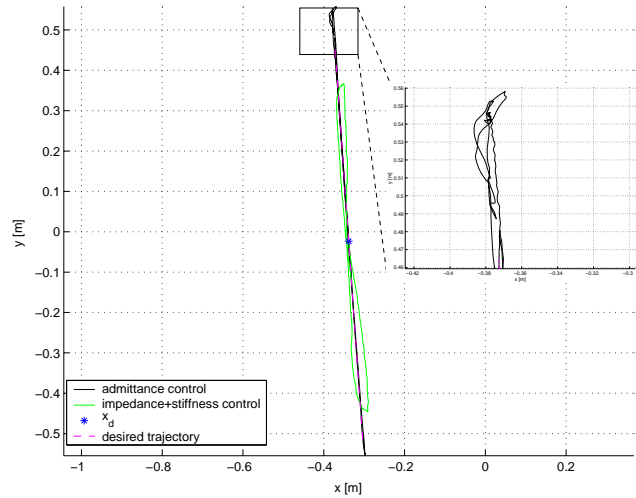


Figure 6: Measurements for admittance control and impedance control enhanced by local stiffness control: x-y plot. The zoomed region corresponds to the singularity

the null-space is not addressed in this paper. Results obtained with the DLR light-weight robot, which are related to these topics are reported in [15]. Nevertheless, it is worth mentioning the implicit behavior in the null-space, resulting from the presented control methods. Both the impedance and the stiffness controller lead to zero stiffness in the null-space. Forces applied in null space direction can move the joints, while keeping the TCP at the same position. The admittance controller is, by contrast, implicitly stiff in the null space. In both cases, the behavior can be changed by explicitly projecting some forces or move-

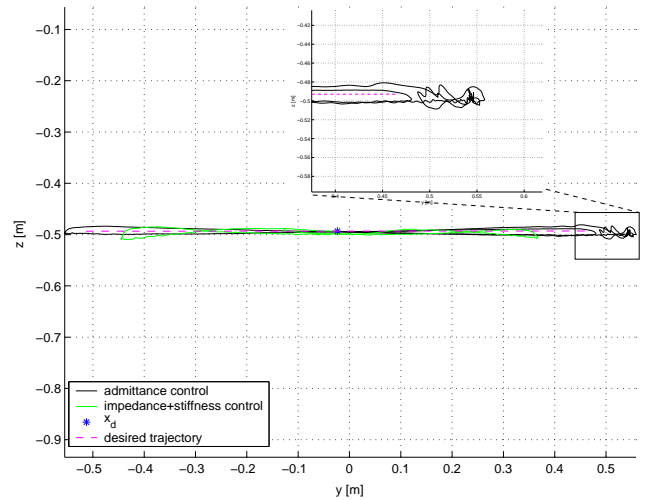


Figure 7: Measurements for admittance control and impedance control enhanced by local stiffness control: y-z plot. The zoomed region corresponds to the singularity

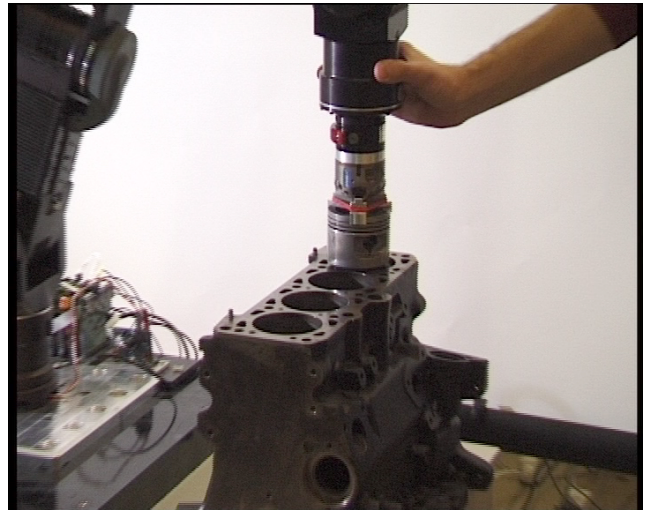


Figure 8: Teaching phase for the automatic piston insertion

ments into the null-space.

6 An application: Automatic piston insertion via teaching by demonstration

As an application for the controller structure proposed in section 4, the task “teaching and automatic insertion of a piston into a motor block” is presented (fig. 8). Teaching is realized by guiding the robot with the human hand, just using the internal torque sensing.

It was initially known that the axes of the holes in

the motor block were vertically oriented. In the teaching phase, high stiffness components for the orientations were commanded, while the translational stiffness was set to zero. This allowed only translational movements to be demonstrated by the human operator.

In the second phase, the taught trajectory has automatically been reproduced by the robot. In this phase, high values were assigned for the translational stiffness, while the stiffness for the rotations was low. This enabled the robot to compensate for the remaining position errors. In this experiment, the assembly was fulfilled automatically four times faster than by the human operator in the teaching phase. For two pistons, the total time for the assembly was 6s. The insertion task had been implemented before using an industrial robot and a compliant force-torque sensor [10]. This experiment in addition focused on the automatic tracking of the motor block by image processing. Despite a well tuned Cartesian force controller, the insertion process had to be performed much slower, because of the well known control problems which occur in case of hard contacts with conventional robots. In this context, the advantage of a compliant manipulator became clear.

Thus it is our strong belief that torque controlled light-weight robots may bring significant advantages, not only in applications which demand mobility, and hence low masses, but also for applications requiring manipulation in contact with unknown environments.

Conclusions

Three different approaches for implementing compliant manipulation were analyzed: impedance, stiffness and admittance control. A new controller structure was proposed, which consists of an impedance controller enhanced by local stiffness control. The presented methods were implemented and compared on DLR's light-weight robots. The proposed controller shows up a better performance than classical impedance and stiffness control. Compared to admittance control, it has lower geometric accuracy, but higher bandwidth and impedance range. As an application for the new controller, the insertion of pistons into a motor block was described; programming times (by directly guiding the robot), and execution times were drastically reduced compared to conventional techniques.

References

[1] D. Abadia. Comparative analysis development of control systems for the DLR light weight robot. Master's thesis, DLR, University of Zaragoza, 2000.

[2] A. Albu-Schäffer and G. Hirzinger. State feedback controller for flexible joint robots: A globally stable approach implemented on DLR's light-weight robots.

IEEE International Conference on Intelligent Robotic Systems, pages 1087–1093, 2000.

[3] A. Albu-Schäffer and G. Hirzinger. Parameter identification and passivity based joint control for a 7DOF torque controlled light weight robot. *IEEE International Conference of Robotics and Automation*, pages 2852–2858, 2001.

[4] F. Caccavale, C. Natale, B. Siciliano, and L. Villani. Six-dof impedance control based on angle/axis representations. *IEEE Transactions on Robotics and Automation*, 15(2):289–299, 1999.

[5] S. Chen and I. Kao. Theory of stiffness control in robotics using the conservative congruence transformation. *International Symposium of Robotics Research*, pages 7–14, 1999.

[6] S. Chen and I. Kao. Simulation of conservative congruence transformation conservative properties in the joint and cartesian spaces. *IEEE International Conference of Robotics and Automation*, pages 1283–1288, 2000.

[7] G. Hirzinger, A. Albu-Schäffer, M. Hähnle, I. Schaefer, and N. Sporer. On a new generation of torque controlled light-weight robots. *IEEE International Conference of Robotics and Automation*, pages 3356–3363, 2001.

[8] N. Hogan. Impedance control: An approach to manipulation, part I - theory, part II - implementation, part III - applications. *Journ. of Dyn. Systems, Measurement and Control*, 107:1–24, 1985.

[9] N. Hogan. Mechanical impedance of single- and multi-articular systems. In J.M. Winters and S. Woo, editors, *Multiple Muscle Systems: Biomechanics and Muscle Organization*, pages 149–163. Springer-Verlag, New York, 1990.

[10] S. Jörg, J. Langwald, C. Natale, J. Stelter, and G. Hirzinger. Flexible robot-assembly using a multi-sensory approach. *IEEE International Conference of Robotics and Automation*, pages 3687–3694, 2000.

[11] O. Khatib. A unified approach for motion and force control of robot manipulators: The operational space formulation. *RA*, RA-3:43–53, 1987.

[12] R. Koeppel and G. Hirzinger. From human arms to a new generation of manipulators: Control and design principles. *ASME Int. Mechanical Engineering Congress*, 2001.

[13] C. Preusche, R. Koeppel, A. Albu-Schäffer, M. Hähnle, N. Sporer, and G. Hirzinger. Design and Haptic Control of a 6 DoF Force-Feedback Device. In *Workshop on Advances in Interactive Multimodal Telepresence Systems*, Munich, Germany, March 2001.

[14] J. K. Salisbury. Active stiffness control of a manipulator in cartesian coordinates. *19th IEEE Conference on Decision and Control*, pages 83–88, 1980.

[15] G. Schreiber, Ch. Ott, and G. Hirzinger. Interactive redundant robotics: Control of the inverted pendulum with nullspace motion. *accepted at IROS*, 2001.

[16] S. Stramigioli and H. Bruyninckx. Geometry and screw theory for constrained and unconstrained robot. *Tutorial at ICRA*, 2001.